

Fifth-Harmonic Generation in Isotropic Media

IVAN V. TOMOV AND MARTIN C. RICHARDSON, MEMBER, IEEE

Abstract—This paper presents a theoretical study of fifth-harmonic generation (FHG) in an isotropic media. Two schemes are discussed—cascade generation in which the fifth harmonic results from successive nonlinear interactions in two separate elements, and direct generation where the fifth harmonic is produced in an isotropic media with third- and fifth-order nonlinear susceptibilities. In the plane-wave approximation almost full conversion of the pumping energy into the fifth harmonic is found to be possible. FHG with a focused Gaussian beam is also investigated. To determine the optimum conditions for FHG in the cascade scheme, the theory of four-wave mixing of light beams with arbitrary confocal parameters and waist locations is developed. In media with third- and fifth-order nonlinearity, the fifth harmonic results from step and direct processes. The interference between these two processes is discussed. Numerical calculations are presented for metal vapor-gas mixtures and Nd:glass laser pumping radiation.

I. INTRODUCTION

METAL VAPORS and inert gases have recently been utilized as efficient nonlinear media for optical harmonic generation and mixing [1]–[3]. Coherent radiation in the UV and VUV has been produced and theoretical considerations predict that this technique can be extended into the soft X-ray range [1], [4]. Up to the present time, all nonlinear frequency conversion techniques have been based on the utilization of both second- and third-order nonlinear processes. However, the high power densities afforded by picosecond laser pulses permit the consideration of higher order nonlinear optical polarizabilities for the generation of still higher order harmonics with greater incremental steps through the frequency spectrum. For the improvement in the efficiencies of these processes, atomic systems should be selected in order to gain maximum advantage from specific relationships between their resonance lines and the interacting frequencies. In addition, the existence of phase-matching conditions is desirable.

It is important to note that in a system using higher order nonlinearity when phase matching for the direct process is achieved, the phase-matching conditions for the step processes produced by lower order nonlinearities as a whole are also fulfilled, even though each step is individually considerably mismatched [5], [6]. If we are interested in increasing the efficiency of higher order nonlinear conversion techniques care must be taken in considering all possible coherent interference effects between the individual step processes and the direct process.

In this paper a detailed theoretical analysis of fifth-harmonic generation (FHG) in an isotropic nonlinear medium is presented. Although FHG has already been experimentally investigated with an Nd:glass laser, relatively low conversion efficien-

cies have been recorded [7]–[9]. In the present case two possible methods of generation are considered. In the first, a system consisting of two separate cascades is employed to generate the fifth harmonic. In the second case, FHG in a medium having third- and fifth-order polarizabilities is investigated. Numerical calculations have been performed for the generation of the fifth harmonic ($\lambda_5 = 0.212 \mu$) of Nd:glass laser radiation which are also applicable to the case of the Nd:YAG laser. The production of powerful radiation having a wavelength of 0.212μ is of interest because this wavelength is close to the VUV limit, and consequently, quartz optics can be employed for further optical processing. In addition, this radiation can also be used in the generation of higher harmonics such as $\lambda_5/3 = 706.7 \text{ \AA}$ and $\lambda_5/5 = 424 \text{ \AA}$.

In Section II, the phase-matching technique is discussed. It is shown that the use of a mixture of more than two gaseous components permits simultaneous phase-matching conditions to be met for more than one nonlinear process in a single cell. This would be very useful in the VUV where technical problems may arise when several different cells are used.

FHG in the cascade of two separate nonlinear conversion media is discussed in Section III. A detailed analysis is made of four-frequency mixing of Gaussian beams with arbitrary confocal parameters. The numerical results show that the most efficient case occurs when equal confocal parameters for all interacting waves are provided.

In Section IV, FHG in a medium with third- and fifth-order nonlinearity is considered. It is found that, in the plane-wave approximation, ~90-percent conversion efficiency is possible. FHG of a focused Gaussian beam is analyzed, and competing processes arising from the existence of third- and fifth-order susceptibilities are discussed.

Many of the results obtained in this paper may be extended for processes of higher order.

II. PHASE-MATCHING TECHNIQUE FOR MULTISTEP PROCESSES

In various gaseous systems, phase matching has been achieved by mixing two components, one having negative dispersion and the other positive dispersion [1]–[3]. In gases and vapors at low pressure the absorption and the variation of the refractive index is significant only in the region of spectral resonances and the continuum. Far from resonance the dispersion is weak. This permits the use of a gaseous system for frequency conversion over a wide spectral range. To date, phase-matching conditions for a single nonlinear process have been realized only for a two-gas (vapor) mixture or for a gas-vapor mixture. It is our intent to show that if a gaseous system of more than two components with suitable resonances is employed, phase-matching conditions for several successive nonlinear processes can be achieved in a single cell. Although

the production of a homogeneous mixture of several metal vapors and gases with specific relative concentrations may pose some problems, already, some progress has been made in this area [10], [11].

Fig. 1 shows the variation of the refractive index n with wavelength for a mixture of sodium, cadmium, and xenon in the ratio 1:2.86:117.5, respectively. This mixture is simultaneously phase matched for the following processes:

$$\begin{aligned} \omega + \omega + \omega &= 3\omega & \omega + \omega + 3\omega &= 5\omega \\ \omega + \omega + \omega + \omega + \omega &= 5\omega \end{aligned} \quad (1)$$

where ω is the frequency of Nd:glass radiation. Note that the resonance line for Na (0.589 μ) is situated between 1.06 and 0.353 μ , and that of Cd (0.229 μ), between 0.353 and 0.212 μ . Xenon is positively dispersive over the region of interest and is added in suitable proportion to compensate for the negative dispersion of the metal vapors. Although a mixture of Na and Xe can provide phase matching for FHG (see Table I) when phase matching for THG is met, the mixture has $n_1 = n_3$ but $n_1 < n_5$ and is consequently positively dispersive from the point of view of FHG. However the addition of Cd which is negatively dispersive provides $n_1 = n_5$. At a temperature $T \approx 555$ K, the ratio of saturated vapor densities of Cd and Na is $N_{Cd}/N_{Na} = 2.86$ and the use of a relatively simple heat pipe is required for the production of phase-matched mixtures. But at this temperature the concentration of sodium atoms, $N_{Na} \approx 10^{14}$ atom/cm³, is too small for good conversion efficiency. The saturated sodium vapor density is $N_{Na} = 10^{17}$ atom/cm³ at $T \approx 810$ K, and then $N_{Cd}/N_{Na} = 3.35$. In this case, a more complicated technique would be required for phase matching since the cadmium vapor would have to be unsaturated. In experiments where tight focusing is employed, the necessary phase-matching ratio will be variable, and some flexibility in operating parameters may be obtained by varying the temperature and focusing conditions. One can expect additional technical problems to arise when different metals are used, since not all combinations of two-metal vapors mix homogeneously [12].

In the mixture considered above, substitute vapors may be possible: sodium can be replaced with some other alkali metal (Na has the smallest absorption at 0.212 μ), cadmium can be replaced with Mg or Zn ($N_{Xe}/N_{Na} = 57$, $N_{Mg}/N_{Na} = 1.65$; $N_{Xe}/N_{Na} = 146$, $N_{Na}/N_{Zn} = 1.87$). Zn is of particular interest because its strongest line (0.2138 μ) is close to the fifth-harmonic wavelength $\lambda_5 = 0.212$ μ .

If we add argon to the mixture of Cd, Na, and Xe, simultaneous phase matching for the processes (1), and the following processes $3\omega + 3\omega + 3\omega = 9\omega$, $\omega + 3\omega + 5\omega = 9\omega$, $\omega + \omega + \omega + \omega + 5\omega = 9\omega$, and $\omega + \omega = 9\omega$ is also possible. In such a mixture the single-photon absorption cross sections for the wavelengths of interest ($\lambda_1 = 1.06$ μ , $\lambda_3 = 0.353$ μ , $\lambda_5 = 0.212$ μ , and $\lambda_9 = 0.1178$ μ) are all less than 0.2 Mbn (0.2×10^{-18} cm²). The ninth harmonic produced will result from the coherent interference of both individual step and direct processes involving odd nonlinear susceptibilities from the third to ninth order. Obviously the way these processes interfere will determine the overall efficiency of the optical convertor.

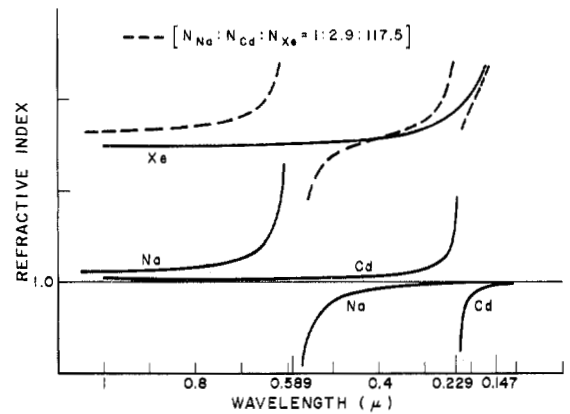


Fig. 1. Refractive indices of Na, Cd, Xe, and mixture of 1 part Na + 2.86 parts Cd + 117.5 parts Xe versus wavelength.

Finally, we note that by suitable arrangement of the configuration of the heat pipe oven, several different zones could be realized, each satisfying phase-matching conditions for different nonlinear processes. For example, in a phase-matched mixture of a metal vapor and an inert gas, the inert gas itself can be a mixture of several gases satisfying other phase-matching conditions. In addition, it may be possible to locate, in one heat pipe oven, several different, physically separated zones of metal vapor-gas mixtures.

III. FHG IN TWO SEPARATE STEPS

Nonlinearities of second, third, and fourth orders may be employed to generate the fifth harmonic in a cascade system [6]–[9]. Phase matching for each step is provided in separate nonlinear elements. Several combinations are possible. Here we will discuss two of them in which an isotropic nonlinear media is employed in at least the final step:

- 1) first step: tripling $\omega + \omega + \omega = 3\omega$, and second step: mixing $\omega + \omega + 3\omega = 5\omega$;
- 2) first step: doubling $\omega + \omega = 2\omega$, and second step: mixing $\omega + 2\omega + 2\omega = 5\omega$.

For a plane-wave approximation [13]

$$E_j = A_j \exp(i\omega_j t - ik_j z). \quad (2)$$

Each one of the above processes can separately permit 100-percent conversion efficiency. To achieve maximum efficiency for the combination of two processes, additional requirements have to be met. Without detailed analysis, we will determine the conditions for full conversion of the fundamental radiation to its fifth harmonic for both schemes.

A. Plane-Wave Approximation

We assume that in both steps an optimal relation between the phases of the interacting waves exists. At the input of the two-step system it is assumed that $A_1(0) = A_{10}$, $A_2(0) = A_3(0) = A_5(0) = 0$ (here the subscripts 1, 2, 3, and 5 refer to the wave with frequencies ω , 2ω , 3ω , and 5ω , respectively).

First we discuss scheme 1). At the output of the first step ($z = L_1$) we have for the amplitudes

$$A_1(L_1) = \frac{A_{10}}{\sqrt{1 + L_1^2/L_{30}^2}} \quad A_3(L_1) = \frac{A_{10} L_1/L_{30}}{\sqrt{1 + L_1^2/L_{30}^2}} \quad (3)$$

where

$$\begin{aligned} L_1 & \text{ length of the first nonlinear element;} \\ \sigma_3 & = 18\pi\omega^2\chi^{(3)}/k_3c^2; \\ c & \text{ velocity of light;} \\ \chi^{(3)} & \text{ nonlinear susceptibility of the third} \\ & \text{ order for the process } \omega + \omega + \omega = 3\omega; \\ L_{30} & = (\sigma_3 A_{10}^2)^{-1} \text{ characteristic interaction length;} \end{aligned}$$

and at $L_1/L_{30} = 3$, $A_3(L_1) = 0.95 A_{10}$.

We assume linearly polarized light waves in the same direction; then the vector nature of the electric field as well as the tensor nature of the nonlinear susceptibilities may be neglected. The amplitudes of the interacting waves in the second step are described (in the slowly varying envelope approximation) by the coupled wave equations

$$\begin{aligned} \frac{dA_1}{dz} & = -2\sigma_3' A_1 A_3 A_5 & \frac{dA_3}{dz} & = -3\sigma_3' A_1^2 A_5 \\ \frac{dA_5}{dz} & = 5\sigma_3' A_1^2 A_3 \end{aligned} \quad (4)$$

where

$$\sigma_3' = 2\pi\omega^2\chi^{(3)}/k_1c^2.$$

It should be noted that the nonlinear susceptibilities $\chi^{(3)}$ and $\chi^{(3)prime}$ may be significantly different since in the mixing process we have three different frequencies which may permit more optimum use of upper atomic levels. The features of the solution of (4) are determined by the ratio $A_1(L_1)/A_3(L_1)$. Full conversion efficiency of the two-cascade system is obtained when, at the input to the second step one has

$$A_1^2(L_1) = 0.4 A_{10}^2 \quad A_3^2(L_1) = 0.6 A_{10}^2. \quad (5)$$

In this case the second-step output amplitudes are

$$\begin{aligned} A_1(L_2) & = \sqrt{0.4} \frac{A_{10}}{\sqrt{1 + L_2^2/L_{20}^2}} \\ A_3(L_2) & = \sqrt{0.6} \frac{A_{10}}{\sqrt{1 + L_2^2/L_{20}^2}} \\ A_5(L_2) & = \frac{A_{10}L_2/L_{20}}{\sqrt{1 + L_2^2/L_{20}^2}}, \end{aligned} \quad (6)$$

here

$$L_{20} = (\sqrt{12/5} \sigma_3' A_{10}^2)^{-1}.$$

Obviously when $L_2/L_{20} \gg 1$ one has $A_5(L_2) \simeq A_{10}$, and all fundamental wave energy is converted into its fifth harmonic.

When the same analysis is applied to the second scheme it is found that full conversion efficiency is achieved when after the first step (doubling) the amplitudes are

$$A_1^2(L_1) = 0.2 A_{10}^2 \quad A_2^2(L_1) = 0.8 A_{10}^2 \quad (7)$$

The physical interpretation of (5) and (7) is quite clear in photon terminology: (5) shows that at the input of the second step, the number of photons with energy $3\hbar\omega$ must be a half-integral of those with energy $\hbar\omega$, since in every elementary interaction one $3\hbar\omega$ photon is coupled with two $\hbar\omega$ photons and produces a $5\hbar\omega$ photon. Similarly, from (7), the number of photons with energy $2\hbar\omega$ should be twice those of $\hbar\omega$.

Calculated phase-matched ratios in a mixture of xenon and some metal vapors are presented in Table I for the type of interactions considered here.

B. Four-Wave Mixing by Gaussian Beams

The high power densities required for efficient higher order nonlinear processes in vapors and gases are achieved by focusing. Since second-harmonic generation (SHG) and third-harmonic generation (THG) in focused beams have been studied in detail elsewhere [14]–[17], only four-wave mixing which takes place in the second step will be treated in detail here. Bjorklund [18] has recently presented a rigorous treatment of four-wave mixing in an isotropic medium. In his analysis, identical confocal parameters and identical waist locations for all fundamental light beams were assumed. Here we extend this treatment to include the cases of interacting beams with arbitrary confocal parameters and different waist locations. In mixing experiments the wavelengths of the interacting beams may differ considerably, and with equal confocal parameters ($b_j = k_j w_{j0}^2$) the short-wavelength beam will spatially overlap a smaller region of the longer wavelength beam. This might suggest that the signal power could be increased if the volumes of the focal regions are more equal for all three beams.

In addition it is necessary to determine how critically the output signal power depends upon the mismatch between focal spot positions of the interacting beams. These two points will now be addressed for the second step of the FHG cascade.

We will study the process of four-wave mixing $\omega_\alpha + \omega_\beta + \omega_\gamma = \omega_s$ with wave vectors

$$k_\alpha + k_\beta + k_\gamma = k_s + \Delta, \quad (|\Delta| \ll k_j), \quad j = \alpha, \beta, \gamma. \quad (8)$$

The fundamental beams at ω_α , ω_β , and ω_γ are assumed to be lowest order Gaussian modes which propagate concentrically along the z axis oriented normally to the nonlinear media surface as in Fig. 2. The cross section of nonlinear media is considered infinite relative to the beam diameter. Similar refractive indices for both linear and nonlinear media are assumed. If a Gaussian beam passes through a thin spherical lens located at $z = 0$, then the amplitude of the beam is described by the expression

$$A_j(x, y, 0) = A_{j0} \exp \left[-(x^2 + y^2) \left(\frac{1}{w_j^2} - \frac{ik_j}{2R_j} \right) \right]. \quad (9)$$

Here w_j is the radius of the beam, R_j is the radius of the beam wavefront after passing through the lens. It is defined by the curvature of the wavefront before the lens and the focal length of the lens. The three fundamental beams propagate along the z axis and may have arbitrary confocal parameters and arbitrary waist locations. The absorption for all frequencies and the depletion of the fundamental beam amplitudes by the nonlinear process are neglected.

Under these assumptions the propagation of a Gaussian beam is described by the equation

$$\left[\frac{\partial}{\partial z} + \frac{i}{2k_j} \left(\frac{\partial^2}{\partial x^2} + \frac{\partial^2}{\partial y^2} \right) \right] A_j = 0. \quad (10)$$

The solution of (10) for the initial condition (9) is

TABLE I
THE PHASE-MATCHED¹ RATIO OF Xe TO METAL ATOMS FOR THG AND
FHG OF Nd:GLASS LASER RADIATION ($\lambda_1 = 1.06 \mu$)

| interaction metal | N_{Xe}/N_{metal} | | | |
|----------------------|----------------------------------|-----------------------------------|------------------------------------|--|
| | $\omega+\omega+\omega = 3\omega$ | $\omega+\omega+3\omega = 5\omega$ | $2\omega+2\omega+\omega = 5\omega$ | $\omega+\omega+\omega+\omega+\omega = 5\omega$ |
| Li | 152.7 | 12.6 | - | 35.3 |
| Na | 150.4 | 9.6 | - | 30.2 |
| K | 325.3 | 31.5 | - | 75.6 |
| Rb | 412.5 | 39.8 | - | 95.8 |
| Cs | 660.7 | 70.9 | 11.8 | 160.1 |
| Ca | 242.4 | - | 58.3 | 31.9 |
| Cd | - | 34.4 | 35.1 | 31.1 |
| Mg | - | 28.7 | 19.1 | 15.6 |
| Zn | - | 255.6 | 243.7 | 215.2 |

¹The refractive index of Xe was derived from the Koch formula [17]; the refractive index of metal vapors was calculated from the standard Sellmeier equation and data as follows: alkali metals [17], Ca [24], Cd [25], Mg [26], Zn [27].

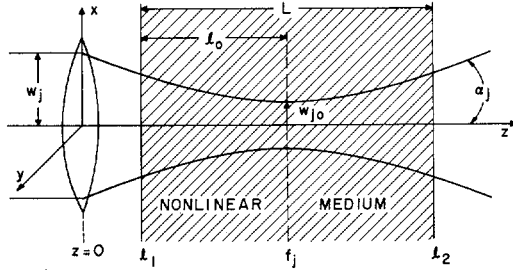


Fig. 2. Fundamental beam focused at $z = f_i$ in an isotropic nonlinear medium. Focal spot radius at f_i is w_{j0} .

$$A_j(x, y, z) = \frac{A_{j0}}{\xi_j(z)} \exp \left[-\frac{x^2 + y^2}{\xi_j(z)} \left(\frac{1}{w_j^2} - \frac{ik_j}{2R_j} \right) \right] \quad (11)$$

where

$$\xi_j(z) = 1 - \frac{z}{R_j} - i \frac{2z}{k_j w_j^2}, \quad |\xi_j(z)|$$

is a dimensionless measure of the beam cross-section variation along the z axis due to focusing and diffraction. If one translates the beginning of the coordinate system to the point f_j (Fig. 2) where the beam cross section is a minimum (focal spot) with the substitution

$$\zeta_j = \frac{2}{b_j} (z - f_j) \quad (12)$$

then

$$A_j(x, y, \zeta_j) = \frac{B_{j0}}{1 - i\zeta_j} \exp \left(-\frac{k_j(x^2 + y^2)}{b_j(1 - i\zeta_j)} \right) \quad (13)$$

where

$$B_{j0} = A_{j0} \left[\left(\frac{2R_j}{k_j w_j^2} - i \right) \frac{b_j}{2R_j} \right]^{-1}$$

is the electric field amplitude at the center of the focal spot $(0, 0, f_j)$ and $b_j = 4/k_j \alpha_j^2 = k_j w_{j0}^2$ is the confocal parameter, α_j being the far-field semiangular spread of the beam.

The equation describing the behavior of the signal amplitude A_s is

$$\left[\frac{\partial}{\partial z} + \frac{i}{2k_s} \left(\frac{\partial^2}{\partial x^2} + \frac{\partial^2}{\partial y^2} \right) \right] A_s = -i\sigma A_\alpha A_\beta A_\gamma \exp(-i\Delta z) \quad (14)$$

where $\sigma = 2\pi\omega_s^2 \chi^{(3)}/k_s c^2$. With the initial conditions, $A_s(x, y, l_1) = 0$, $A_j = A_j(x, y, l_1)$ at the interface $z = l_1$, the solution of (14) is

$$A_s(x, y, z) = -i \frac{\sigma A_{\alpha 0} A_{\beta 0} A_{\gamma 0}}{4} \int_{l_1}^z \frac{\exp \left(-\frac{x^2 + y^2}{4m_1(\tau)} - i\Delta\tau \right) d\tau}{m_1(\tau)m_2(\tau)} \quad (15)$$

where

$$g_j = \frac{1}{\xi_j(\tau)} \left[\frac{1}{w_j^2} - \frac{ik_j}{2R_j} \right] \quad m_1(\tau) = \frac{1}{4(g_\alpha + g_\beta + g_\gamma)} + i \frac{\tau - z}{2k_s},$$

$$m_2(\tau) = \xi_\alpha(\tau) \xi_\beta(\tau) \xi_\gamma(\tau) (g_\alpha + g_\beta + g_\gamma).$$

Integrating over the intensity distribution gives the signal power P_s :

$$P_s = \frac{cn_s}{8\pi} \int_{-\infty}^{\infty} \int_{-\infty}^{\infty} A_s A_s^* dx dy = \frac{128n_s \sigma^2 P_{\alpha 0} P_{\beta 0} P_{\gamma 0}}{c^2 n_\alpha n_\beta n_\gamma w_\alpha^2 w_\beta^2 w_\gamma^2} \times \int_{l_1}^z d\tau \int_{l_1}^z d\tau' \frac{\exp[-i\Delta(\tau - \tau')]}{m_2(\tau) m_2^*(\tau') [m_1(\tau) + m_1^*(\tau')]} \quad (16)$$

$P_{j0} = 16A_{j0} A_{j0}^* / cn_j w_j^2$ is the fundamental beam power at frequency ω_j .

In further calculations we will neglect the difference between indices of refraction except in the expression for Δ .

The expressions for the signal amplitude (15) and signal power (16) can be extended in a very simple way for the other four-wave interactions, such as

1) for the process $\omega_\alpha + \omega_\beta - \omega_\gamma = \omega_s$, $k_\alpha + k_\beta - k_\gamma = k_s + \Delta$ by the following replacement:

$$A_{\gamma 0} \rightarrow A_{\gamma 0}^*, \quad g_\gamma \rightarrow g_\gamma^*, \quad \xi_\gamma \rightarrow \xi_\gamma^*;$$

2) for the process $\omega_\alpha - \omega_\beta - \omega_j = \omega_s$, $k_\alpha - k_\beta - k_\gamma = k_s + \Delta$ by the following replacement:

$$A_{\beta 0} \rightarrow A_{\beta 0}^*, \quad A_{\gamma 0} \rightarrow A_{\gamma 0}^*, \quad g_\beta \rightarrow g_\beta^*, \quad g_\gamma \rightarrow g_\gamma^*,$$

$$\xi_\beta \rightarrow \xi_\beta^*, \quad \xi_\gamma \rightarrow \xi_\gamma^*.$$

Thus the formulas (15) and (16) describe the signal amplitude and the power for all types of four-wave interactions in an isotropic medium between coaxial Gaussian beams with arbitrary confocal parameters and beam waist locations on the z axis.

Simplification of these expressions must be performed explicitly for each experimental situation. It is seen that in most cases the signal is not of a lowest order Gaussian mode.

Here we present in detail the dependence of the sum-mixing power P_s on the beam confocal parameters and on the positions of the beam waists for FHG. Numerical computations have been performed for different values of the parameters of interest. In order to determine the optimum conversion efficiency for a practical system, special attention was paid to the following three situations:

- 1) equal confocal parameters $b_\alpha = b_\beta = b_\gamma$;
- 2) equal cross section of the beam waists $w_{\alpha 0} = w_{\beta 0} = w_{\gamma 0}$.
- 3) equal volume of the beam waist regions $b_\alpha w_{\alpha 0}^2 = b_\beta w_{\beta 0}^2 = b_\gamma w_{\gamma 0}^2$.

For the most efficient of these three configurations, the dependence of the signal power P_s on the relative beam focal spot positions f_j was studied.

For this purpose some new parameters in (16) will be introduced. If the distance between focal spot f_j and input surface (Fig. 2) of the nonlinear medium is l_0 , the parameter $d = l_0/L$ will define the minimum spot size position. The focal points f_β and f_γ are on the z axis and $f_\beta - f_\alpha = \delta_{\beta 0}$, $f_\gamma - f_\alpha = \delta_{\gamma 0}$. $\delta_{\beta 0}$ and $\delta_{\gamma 0}$ are permitted to be either negative or positive depending on the positions of f_β and f_γ relative to f_α .

Substituting

$$\eta = \frac{2}{L}(\tau - f_\alpha) \quad (17)$$

(16) becomes

$$P_s = \frac{128\sigma^2 P_{\alpha 0} P_{\beta 0} P_{\gamma 0} k_\beta k_\gamma (1 + t_\beta + t_\gamma)}{c^2} \cdot q_\beta q_\gamma J_0 \left(d, \frac{\Delta L}{2}, q_j, \delta_l, t_l \right) \quad (18)$$

and

$$J_0 \left(d, \frac{\Delta L}{2}, q_j, \delta_l, t_l \right) = \int_{-2d}^{2(1-d)} d\eta \int_{-2d}^{2(1-d)} d\eta' \frac{\exp \left[-i \frac{\Delta L}{2} (\eta - \eta') \right]}{m_{20}(\eta) m_{20}^*(\eta') [m_{10}(\eta) + m_{10}^*(\eta')]} \quad (19)$$

where

$$m_{10}(x) = \frac{1 + t_\beta + t_\gamma}{(1 - iq_\alpha x)^{-1} + t_\beta q_\beta / q_\alpha (1 - iq_\beta x + i\delta_\beta q_\beta) + t_\gamma q_\gamma / q_\alpha (1 - iq_\gamma x + i\delta_\gamma q_\gamma)} + iq_\alpha x$$

$$m_{20}(x) = (1 - iq_\beta x + i\delta_\beta q_\beta)(1 - iq_\gamma x + i\delta_\gamma q_\gamma)$$

$$+ \frac{q_\alpha}{t_\beta q_\beta} (1 - iq_\alpha x)(1 - iq_\gamma x + i\delta_\gamma q_\gamma)$$

$$+ \frac{q_\alpha}{t_\gamma q_\gamma} (1 - iq_\alpha x)(1 - iq_\beta x + i\delta_\beta q_\beta)$$

$$\delta_l = \frac{2\delta_{l0}}{L}, \quad t_l = \frac{k_l}{k_\alpha}, \quad (j = \alpha, \beta, \gamma, \quad l = \beta, \gamma)$$

$q_j = L/b_j$ is the focusing parameter.

When the confocal parameters are equal ($b_\alpha = b_\beta = b_\gamma$) and the focal spots coincide ($\delta_\beta = \delta_\gamma = 0$), then (19) becomes

$$J_0 \left(d, \frac{\Delta L}{2}, q_\alpha, 0, t_l \right) = \frac{1}{2} (1 + t_\beta + t_\gamma)^{-2} \left| \int_{-2d}^{2(1-d)} \frac{\exp \left(-\frac{i\Delta L}{2} \eta \right) d\eta}{(1 - iq_\alpha \eta)^2} \right|^2 \quad (20)$$

an integral which has been investigated elsewhere [15]–[18]. It should be noted, however, that only in this case is the resulting beam in a single Gaussian mode. For any other configuration a multimode output results due to the mismatch between the size and position of confocal parameters of the interacting beams and the induced polarization.

For the evaluation of J_0 as a function of $\Delta L/2$ for various sets of other parameters we have employed a fast Fourier transform [19]. Numerical calculations of the integral (19) were performed for FHG for the interactions $\omega + \omega + 3\omega = 5\omega$ and $\omega + 2\omega + 2\omega = 5\omega$. In the expressions to follow the indices α, β, γ , and s will be replaced by 1, 2, 3, and 5 for the fundamental, second harmonic, third harmonic, and fifth harmonic, respectively. In the first interaction the two waves of the fundamental frequency are identical, thus $t_\beta = 1$, $t_\gamma = 3$, $q_1 = q_\beta$, and $\delta_\beta = 0$. We believe, as pointed out in [17], that when tight focusing is employed and the focus position is far enough from both ends of the nonlinear medium ($1/q_j < d < 1 - 1/q_j$), the value of J_0 is almost independent of the exact position of the focus. In our calculation, $d = \frac{1}{2}$ was chosen. The calculated products $q_1 q_3 J_0$ are plotted in Fig. 3 for the confocal parameter $q_1 = 20$ and the step $\delta(\Delta L/2) = \pi$. To obtain the confocal parameter configuration mentioned above the confocal parameter of the third harmonic and its waist location were changed as indicated in the corresponding curves in Fig. 3. In curve $q_3 = 20$ the maximum value occurs at $\Delta L/2 \approx 6\pi$ which corresponds to $\Delta \approx 2/b_1$ obtained from the analytical approximation for infinitely tight focusing. The maximum of $q_1 q_3 J_0$ at given confocal parameters moves towards smaller values of $\Delta L/2$ when $q_3 < q_1$ and towards larger values of $\Delta L/2$ when $q_3 > q_1$. In both cases its absolute value decreases.

For equal confocal parameters $q_1 = q_3 = 20$ we have calculated the influence of the focal spot mismatch on the

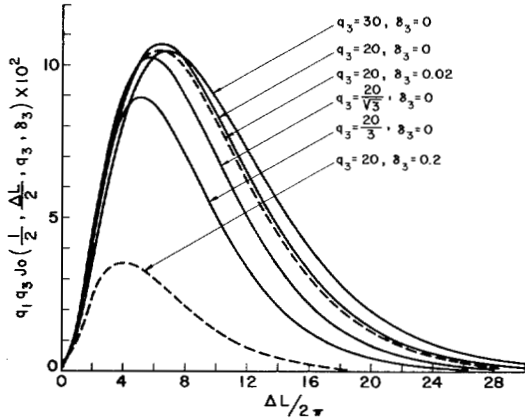


Fig. 3. Function $q_1 q_3 J_0$ versus $\Delta L/2\pi$ for sum-mixing $\omega + \omega + 3\omega = 5\omega$. $q_1 = q_3 = 20$. Curve $q_3 = 20$, corresponds to equal confocal parameters; $q_3 = 20/3$, equal cross sections of the beam waists; $q_3 = 20/\sqrt{3}$, equal beam waist volumes.

signal power. Two curves are shown in Fig. 3. For $\delta_3 = 0.02$ the maximum of $q_1 q_3 J_0$ decreases by ~ 3 percent and at $\delta_3 = 0.2$, $q_1 q_3 J_0$ is ~ 30 percent of its optimum value. From these and other calculations with different δ_3 we conclude that the accuracy of coincidence of the focal spots for ω and 3ω needs to be better than $0.1 b_1$.

Fig. 4 presents the results for $q_1 = 1$. The maximum value of $q_1 q_3 J_0$ occurs again for equal confocal parameters $q_1 = q_3 = 1$. For weaker focusing the sidelobe structure is more evident. It was found that $q_1 q_3 J_0$ decreases less than 2 percent when a mismatch $\delta_2 = 0.2$ was included. Thus one can expect that with weaker focusing conditions the influence of focal spots mismatch will decrease.

The results for the interaction $\omega + 2\omega + 2\omega = 5\omega$ are plotted in Fig. 5. Here $t_\beta = t_\gamma = 2$, $q_\beta = q_\gamma = q_2$, and $\delta_\beta = \delta_\gamma$. It should be noted that the curve with $q_1 = q_3 = 20$ is the same for both interactions as follows from (20). With variation of the parameters q_2 and δ_2 the behavior of $q_2^2 J_0$ is similar to that for the interaction $\omega + \omega + 2\omega = 5\omega$. The same accuracy of focal spot coincidence as above is also required.

Thus it is seen from these calculations that the fifth-harmonic power has its maximum value for equal confocal parameters. Although we have no analytical proof we believe this to be the general case for the four-wave sum-mixing process.

IV. FHG IN ISOTROPIC MEDIA WITH THIRD- AND FIFTH-ORDER NONLINEARITY

In this section FHG in an isotropic medium with nonlinear polarization expressed as

$$P^{NL} = \chi^{(3)} EEE + \chi^{(5)} EEEEE \quad (21)$$

will be considered.

In such a medium the fifth harmonic results from two simultaneous processes:

- 1) the step processes involving the third-order nonlinearity

$$\omega + \omega + \omega = 3\omega \quad \text{and} \quad \omega + \omega + 3\omega = 5\omega$$

$$k_1 + k_1 + k_1 = k_3 + \Delta_{13} \quad k_1 + k_1 + k_3 = k_5 + \Delta_{135} \quad (22)$$

- 2) the direct process involving the fifth-order nonlinearity

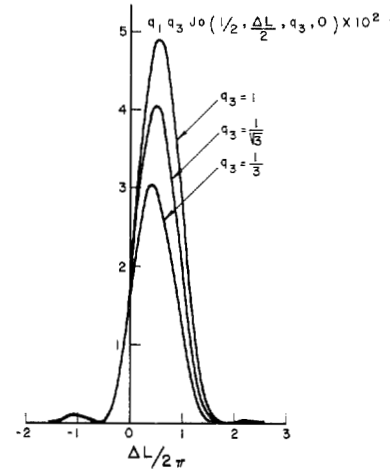


Fig. 4. Function $q_1 q_3 J_0$ versus $\Delta L/2\pi$ for sum-mixing $\omega + \omega + 3\omega = 5\omega$, $q_1 = q_3 = 1$. Curve $q_3 = 1$ corresponds to equal confocal parameters, $q_3 = 1/3$, equal cross section of the beam waists; $q_3 = 1/\sqrt{3}$, equal beam waist volumes.

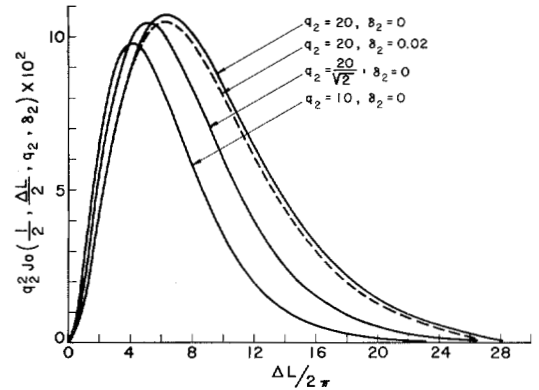


Fig. 5. Function $q_2^2 J_0$ versus $\Delta L/2\pi$ for sum-mixing $\omega + 2\omega + 2\omega = 5\omega$. $q_1 = 20$. Curve $q_2 = 20$ corresponds to equal confocal parameters; $q_2 = 10$, equal cross section of the beam waists; $q_2 = 20/\sqrt{2}$, equal beam waist volumes.

$$\omega + \omega + \omega + \omega + \omega = 5\omega,$$

$$k_1 + k_1 + k_1 + k_1 + k_1 = k_5 + \Delta_{15} \quad (23)$$

where, obviously, $\Delta_{13} + \Delta_{135} = \Delta_{15}$.

We have shown in Section II that with the use of suitable combinations of vapors and gases, it is possible to obtain different values of the wave-vector mismatch including $\Delta_{13} = \Delta_{135} = \Delta_{15} = 0$. In Section III-A it was found that when the cascade system is used it is possible to convert all the energy of the fundamental frequency to its fifth harmonic. It is therefore interesting to determine what the maximum conversion efficiency would be for only a single cell having nonlinear polarizability described by (21), under the same plane-wave approximation.

4. Plane-Wave Approximation

From Maxwell's equation for a lossless nonlinear medium, with a polarizability expressed by (21), the following set of differential equations for coupled amplitudes of the interacting waves are obtained [13]:

$$\begin{aligned}\frac{dA_1}{dz} &= -i\sigma_1 A_1^{*2} A_3 \exp i\Delta_{13}z - i\sigma'_1 A_1^{*4} A_5 \exp i\Delta_{15}z \\ &\quad - i\sigma''_1 A_1^* A_3^* A_5 \exp i\Delta_{135}z \\ \frac{dA_3}{dz} &= -i\sigma_3 A_1^3 \exp -i\Delta_{13}z - i\sigma_2 A_1^{*2} A_5 \exp i\Delta_{135}z \\ \frac{dA_5}{dz} &= -i\sigma_5 A_1^5 \exp -i\Delta_{15}z - i\sigma_4 A_1^2 A_3 \exp -i\Delta_{135}z\end{aligned}\quad (24)$$

where

$$\begin{aligned}\sigma_1 &= 6\pi\omega\chi^{(3)}/cn_1, & \sigma_3 &= 6\pi\omega\chi^{(3)}/cn_3, \\ \sigma''_1 &= 4\pi\omega\chi'^{(3)}/cn_1, & \sigma_2 &= 6\pi\omega\chi'^{(3)}/cn_3, \\ \sigma_4 &= 10\pi\omega\chi'^{(3)}/cn_5, & \sigma'_1 &= 10\pi\omega\chi^{(5)}/cn_1, \\ \sigma_5 &= 10\pi\omega\chi^{(5)}/cn_5.\end{aligned}$$

We have performed a numerical integration of (24), which has been verified by using the usual energy balance equation for a lossless medium:

$$|A_1(z)|^2 + |A_3(z)|^2 + |A_5(z)|^2 = \text{constant} \quad (25)$$

to an accuracy of better than 1 percent. Numerical integration is possible in complex numbers but, in the present case, the following procedure was adopted. Introducing the real amplitude and phase of the waves, then

$$A_j(z) = A'_j(z) \exp(i\theta_j(z)) \quad (26)$$

and through normalization

$$a_j(z) = A'_j(z)/A'_1(0) \quad \tilde{z} = z\sigma_3 A_1'^2(0) = z/L_{30}.$$

The coupled amplitude equations (24) then become

$$\begin{aligned}\frac{da_1}{d\tilde{z}} &= -\sigma_{10} a_1^2 a_3 \sin \phi - \sigma'_{10} a_1^4 a_5 \sin \psi - \sigma''_{10} a_1 a_3 a_5 \\ &\quad \cdot \sin(\psi - \phi) \\ \frac{da_3}{d\tilde{z}} &= a_1^3 \sin \phi - \sigma_{20} a_1^2 a_5 \sin(\psi - \phi) \\ \frac{da_5}{d\tilde{z}} &= \sigma_{50} a_1^5 \sin \psi + \sigma_{40} a_1^2 a_3 \sin(\psi - \phi) \\ \frac{d\phi}{d\tilde{z}} + \tilde{\Delta}_{13} &= (a_1^3/a_3 - 3\sigma_{10} a_1 a_3) \cos \phi - 3\sigma'_{10} a_1^3 a_5 \cos \psi \\ &\quad + (\sigma_{20} a_1^2 a_5/a_3 - 3\sigma''_{10} a_3 a_5) \cos(\psi - \phi) \\ \frac{d\psi}{d\tilde{z}} + \tilde{\Delta}_{15} &= -5\sigma_{10} a_1 a_3 \cos \phi + (\sigma_{50} a_1^5/a_5 - 5\sigma'_{10} a_1^3 a_5) \\ &\quad \cdot \cos \psi + (\sigma_{40} a_1^3 a_3/a_5 - 5\sigma''_{10} a_3 a_5) \cos(\psi - \phi)\end{aligned}\quad (27)$$

where

$$\begin{aligned}\tilde{\Delta}_{13} &= \Delta_{13}/\sigma_3 A_{10}'^2, & \tilde{\Delta}_{15} &= \Delta_{15}/\sigma_3 A_{10}'^2, \\ \sigma_{10} &= \sigma_1/\sigma_3, & \sigma_{20} &= \sigma_2/\sigma_3, \\ \sigma_{40} &= \sigma_4/\sigma_3, & \sigma''_{10} &= \sigma''_1/\sigma_3,\end{aligned}$$

$$\begin{aligned}\sigma'_{10} &= \sigma'_1 A_{10}'^2/\sigma_3, & \sigma_{50} &= \sigma_5 A_{10}'^2/\sigma_3, \\ \phi &= 3\theta_1 - \theta_3 - \Delta_{13}z, & \psi &= 5\theta_1 - \theta_5 - \Delta_{15}z.\end{aligned}$$

These equations have been numerically integrated for parameters corresponding to a nonlinear medium consisting of a mixture of Na, Cd, and Xe. Difficulties arose in defining some of these parameters due to a lack of knowledge of the principle nonlinear susceptibilities. We assume the atomic susceptibilities $\chi_a^{(3)} = \chi_a'^{(3)} = 8.5 \times 10^{-34}$ ESU, calculated by Eicher [20] for tripling of $\lambda = 1.06 \mu$ in Na. In addition we note that in a mixture of Na + Cd + Xe the contribution to $\chi^{(3)}$ and $\chi'^{(3)}$ from Xe atoms can be neglected but the contribution from Cd atoms might be comparable and even greater than that of Na atoms, especially in $\chi'^{(3)}$. Much more uncertainty arises in $\chi^{(5)}$. FHG in gases was reported by Harris [4] but no estimates of $\chi^{(5)}$ were given. Calculations using perturbation theory have yielded for sodium $\chi_a^{(5)} = 6.7 \times 10^{-45}$ ESU [21]. In the present case, for lack of better values, we will assume similar values for susceptibilities $\chi_a^{(3)}$, $\chi_a'^{(3)}$, and $\chi_a^{(5)}$ for Cd and Na. Thus, for a fundamental power density of 2×10^{11} W/cm² (limited in the case of Na by multiphoton ionization [2]) one obtains

$$\begin{aligned}\sigma_{10} = \sigma_{20} &= 1, & \sigma''_{10} &= 0.667, \\ \sigma_{40} &= 1.667, & \sigma'_{10} = \sigma_{50} &= 0.0221, \\ L_{30} &= (\sigma_3 A_1'^2(0))^{-1} = 6.3 \text{ cm}, & (N &= 10^{17} \text{ atom/cm}^3), \\ L_{50} &= (\sigma_5 A_1'^4(0))^{-1} = 283.6 \text{ cm}.\end{aligned}$$

In addition $\sigma_{10} = \sigma_{50} = 1$ and $L_{30} = L_{50} = 0.14$ cm when the power density is 9.1×10^{12} W/cm².

The following initial conditions were assumed:

$$a_1(0) = 1, \quad a_3(0) = a_5(0) = 10^{-5}, \quad \phi(0) = \psi(0) = 0.$$

The solution of (27) for $\tilde{\Delta}_{13} = \tilde{\Delta}_{15} = 0$ and $\sigma'_{10} = \sigma_{50} = 0.0221$ is shown in Fig. 6(a). The third-harmonic amplitude reaches its first maximum, $a_3 = 0.6$, at $\tilde{z} = 1.3$ and the fifth harmonic reaches its first maximum, $a_5 = 0.89$, at $\tilde{z} = 7$. We have calculated the amplitudes for $\tilde{z} \leq 130$, but experimental conditions limit practical values of $\tilde{z} \leq 10$, and hence, only the dependence of the normalized amplitudes is presented for small values of \tilde{z} . Although there is a periodic exchange of energy between interacting waves, a simple periodic function does not always exist due to the competition of both step-wise and direct processes. For example at $\tilde{z} = 62.8$, $a_3 = 0.95$ and at $\tilde{z} = 103.2$, $a_5 = 0.97$. To compare the contribution of step and direct processes we have calculated the amplitudes for the case when $\sigma'_{10} = \sigma_{50} = 0$ (this is the situation when $\chi^{(5)} = 0$). The difference between solutions for both cases is less than 10 percent for $\tilde{z} < 10$. For larger \tilde{z} , significant differences exist. To explain this we note that the growth of the fifth harmonic resulting from the step processes depends on z/L_{30} , whereas the growth of the fifth harmonic resulting from the direct process depends on z/L_{50} . In Fig. 6(a), $L_{30}/L_{50} = 0.0221$ and substantial influence of the direct process will appear only at longer \tilde{z} .

When the power density is increased to a value permitting $\sigma'_{10} = \sigma_{50} = 1$ [(Fig. 6(b))], the normalized amplitude of the

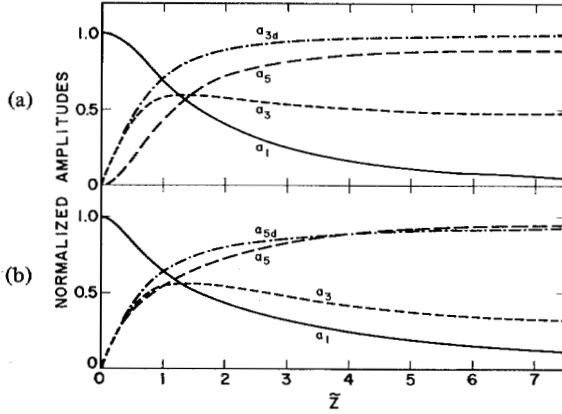


Fig. 6. Variation of normalized fundamental, third, and fifth-harmonic amplitudes for perfect phase matching $\tilde{\Delta}_{13} = \tilde{\Delta}_{15} = 0$. (a) $\sigma'_{10} = \sigma_{50} = 0.0221$, (b) $\sigma'_{10} = \sigma_{50} = 1$. Curves a_{3d} and a_{5d} represent the growth of the third and fifth harmonics by the direct process only. Note that $\tilde{z} = z/L_{30}$ and in (a) $L_{30}/L_{50} = 0.0221$, but in (b) $L_{30}/L_{50} = 1$.

fifth harmonic is $a_5 = 0.94$ at $\tilde{z} = 7$. This corresponds to an energy conversion efficiency of 90 percent. Comparing both Fig. 6(a) and Fig. 6(b) one can observe the difference in growth of a_5 due to the different ratio of L_{30}/L_{50} . We note that the higher order harmonics are growing slower than those of lower order even in a single direct process. For example if every harmonic is generated only in a direct process then the growth of the normalized harmonic amplitude from zero with the normalized distance $\tilde{z}_n = z \sigma_n A_{10}^{n-1}$ is at $\tilde{z} < 0.5$ (and $a_{nd} < 0.4$, $a_1 > 0.9$) almost the same for all harmonics up to the fifth. However the value $a_{nd} = 0.894$ is reached for the second harmonic at $\tilde{z}_2 = 1.44$, third harmonic at $\tilde{z}_3 = 2$, fourth harmonic at $\tilde{z}_4 = 2.95$, and fifth harmonic at $\tilde{z}_5 = 4.67$. The exact functions $a_{3d}(\tilde{z})$ and $a_{5d}(\tilde{z})$ are shown in Fig. 6.

In Fig. 7(a) the amplitude growth for $\sigma'_{10} = \sigma_{50} = 0.0221$, $\tilde{\Delta}_{15} = 0$, $\tilde{\Delta}_{13} = -4.54$, and $\tilde{\Delta}_{13} = -9.32$ are shown. $\tilde{\Delta}_{13} = -4.54$ corresponds to a mixture of Na + Cd + Xe with $T \approx 810$ K having saturated Na and Cd vapor concentrations with $N_{Cd}/N_{Na} = 3.35$ and $N_{Na} = 10^{17}$ atom/cm³. $\tilde{\Delta}_{13} = -9.32$ corresponds to a Cd + Xe mixture with $N_{Cd} = 10^{17}$ atom/cm³. In Fig. 7(b) the same parameters as in Fig. 7(a) are employed, except that $\sigma'_{10} = \sigma_{50} = 1$. In the case of Fig. 7(a) the step processes are more important and the third harmonic changes periodically. Decreasing $\tilde{\Delta}_{13}$ leads to a significant improvement in a_5 . In Fig. 7(b) the direct process is comparable with the step process and even at larger $\tilde{\Delta}_{13} = -9.32$, a_5 is higher. In this case the interference between step and direct processes is substantial for the fifth-harmonic amplitude.

In a phase-matched mixture of Na + Xe for third-harmonic generation ($\tilde{\Delta}_{13} = 0$) $\tilde{\Delta}_{15} = -173.5$, the maximum value of a_5 is less than 3.5×10^{-3} and $a_3(\tilde{z}) \rightarrow 1$ when $\tilde{z} \gg 1$ following (3).

The important result from these calculations is that in a single cell of isotropic media, phase matched for step and direct processes ($\tilde{\Delta}_{13} = \tilde{\Delta}_{15} = 0$), the conversion efficiency of fundamental radiation into its fifth harmonic is comparable to that obtained in a cascade scheme. In a cell with a Cd + Na + Xe mixture with variable Xe concentration, it is possible to obtain $\tilde{\Delta}_{13} = 0$ and generate the third harmonic, or $\tilde{\Delta}_{13} =$

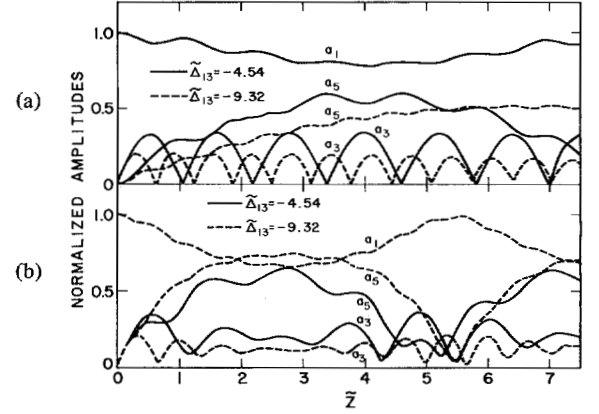


Fig. 7. Variation of the normalized amplitude of the fundamental, third, and fifth harmonics for $\tilde{\Delta}_{15} = 0$, $\tilde{\Delta}_{13} = -4.54$ and $\tilde{\Delta}_{13} = -9.32$. (a) $\sigma'_{10} = \sigma_{50} = 0.0221$, (b) $\sigma'_{10} = \sigma_{50} = 1$.

$\tilde{\Delta}_{15} = 0$ and generate the fifth harmonic. It should be noted that in the above analysis we have not discussed the case when different signs of $\chi^{(3)}$, $\chi'^{(3)}$, and $\chi^{(5)}$ exist because of the lack of experimental or theoretical data.

B. FHG by Focused Gaussian Beam

To extend (24) for a light beam with finite cross section, transverse derivatives should be included. However, some simplifications are necessary to permit analytical solution. We will thus neglect depletion of the fundamental amplitude, (hence $A_1(z) = \text{constant}$) and also the term $\sigma_2 A_1^* A_5$ in the second equation of (24) (this term describes the depletion of the third harmonic arising from its partial conversion into the fifth harmonic). Under these assumptions, FHG is described by the following set of partial differential equations:

$$\begin{aligned} \left[\frac{\partial}{\partial z} + \frac{i}{2k_1} \left(\frac{\partial^2}{\partial x^2} + \frac{\partial^2}{\partial y^2} \right) \right] A_1 &= 0 \\ \left[\frac{\partial}{\partial z} + \frac{i}{2k_3} \left(\frac{\partial^2}{\partial x^2} + \frac{\partial^2}{\partial y^2} \right) \right] A_3 &= -i\sigma_3 A_1^3 \exp -i\Delta_{13}z \\ \left[\frac{\partial}{\partial z} + \frac{i}{2k_5} \left(\frac{\partial^2}{\partial x^2} + \frac{\partial^2}{\partial y^2} \right) \right] A_5 &= -i\sigma_5 A_1^5 \\ &\quad \cdot \exp -i\Delta_{15}z - i\sigma_4 A_1^2 A_3 \exp -i\Delta_{135}z. \end{aligned} \quad (28)$$

The initial conditions are $A_1(x, y, 0)$ from (9) and $A_3(x, y, l_1) = A_5(x, y, l_1) = 0$ (see Fig. 2).

Without focusing of the pumping beam [$R = \infty$ in (9)] and negligible diffraction for fifth-harmonic amplitude we obtain

$$\begin{aligned} A_5(x, y, z) &= A_{10}^5 \exp \left(-5 \frac{x^2 + y^2}{w_f^2} \right) \\ &\quad \cdot \left[\frac{(\sigma_5 + \sigma_3 \sigma_4 / \Delta_{13}) \exp(-i\Delta_{15}z) - 1}{\Delta_{15}} \right. \\ &\quad \left. - \frac{\sigma_3 \sigma_4 \exp(-i\Delta_{135}z) - 1}{\Delta_{13} \Delta_{135}} \right] \end{aligned} \quad (29)$$

and therefore the effective fifth-order nonlinear susceptibility is

$$\chi_{\text{eff}}^{(5)} = \chi^{(5)} + 2\pi \chi^{(3)} \chi'^{(3)} / n_3(n_1 - n_3). \quad (30)$$

We recall that in gases and vapors it is possible that the values of $\chi^{(3)}$ and $\chi'^{(3)}$ are different. Note that the oscillator strengths among the electronic states of an atom and the resonance enhancements which are most responsible for the values of $\chi^{(3)}$ and $\chi'^{(3)}$ are also responsible for the value of $\chi^{(5)}$. A resonance of twice the pump frequency is particularly desirable since it will increase all these nonlinear susceptibilities. As seen from (20) the relative signs of $\chi^{(3)}$, $\chi'^{(3)}$, $\chi^{(5)}$, and $(n_1 - n_3)$ are important. Atoms with approximately equal absolute values of susceptibilities and dispersion, but different signs, would have different values of $\chi_{\text{eff}}^{(5)}$. For example in a mixture of Xe + Na, when $n_1 = n_5$, $n_1 - n_3 > 0$ and in a mixture of Xe + Cd, when $n_1 = n_5$, $n_1 - n_3 < 0$.

Successive solution of (28) substituting (17) gives for the fifth-harmonic amplitude

$$A_5(x, y, l_2) = -i \frac{\sigma_5 L B_{10} \exp(-i\Delta_{15} f_1)}{2(1 - iq_1)} \cdot \exp\left(-\frac{5k_1(x^2 + y^2)}{b_1(1 - iq_1)}\right) J_1 \quad (31)$$

$$J_1(\Delta_{15}L/2, \Delta_{13}L/2, W, q_1, d) = \int_{-2d}^{2(1-d)} \frac{\exp(-i\Delta_{15}L\eta/2) d\eta}{(1 - iq_1\eta)^4} - iWL \int_{-2d}^{2(1-d)} \frac{\exp(-i\Delta_{135}L\eta/2) d\eta}{(1 - iq\eta)^2} \int_{-2d}^{\eta} \frac{\exp(-i\Delta_{13}L\tau/2) d\tau}{(1 - iq_1\tau)^2} = J_d - iWLJ_s. \quad (32)$$

Here $W = \sigma_3\sigma_4/2\sigma_5$. Then for the fifth-harmonic power we obtain

$$P_5 = \frac{32 \cdot 768 k_1^4 P_{10}^5 \sigma_5^2 q_1^2}{5c^4 n_1^4 b_1^2} |J_1|^2. \quad (33)$$

The fifth-harmonic power is governed by the integral (32) and its optimization will now be discussed. The first integral J_d in (32) results from the direct process and the second integral J_s from the step processes. The total value of J_1 depends also on the value and the sign of W which is the ratio between the nonlinear susceptibilities of the third and fifth orders:

$$W = 6\pi^2 N \chi_a^{(3)} \chi_a'^{(3)} / n_3 \lambda_1 \chi_a^{(5)}.$$

For $N = 10^{17}$ atom/cm³, $\lambda_1 = 1.06 \times 10^{-4}$ cm, and the above-cited values of $\chi_a^{(3)}$, $\chi_a'^{(3)}$, and $\chi_a^{(5)}$ we obtain $W = 6.02$ cm⁻¹. For weak focusing $q_1 < 1$, and the maximum fifth-harmonic power is obtained for phase-matching conditions $\Delta_{13} = \Delta_{15} = 0$. Then the integrals in (32) may be performed to give

$$J_1 = \frac{6 - 8q_1^2(1 - 3d + 3d^2) - i12q_1(1 - 2d) - i6WL(1 - i2q_1d)(1 - i2q_1 + i2q_1d)}{3(1 + i2q_1d)^3(1 - i2q_1(1 - d))^3}. \quad (34)$$

At $d = \frac{1}{2}$, the function J_1 reaches the maximum values for both its integrals:

$$J_1 = 2(1 - q_1^3/3 - iWL(1 + q_1^2))/(1 + q_1^2)^3.$$

With strong focusing, $q_1 > 1$ because of the phase shift in the waist region for optimum conversion efficiency some wavevector mismatch Δ_{jk} should be introduced to compensate for this shift. Before evaluation of (32), some analytical approxi-

mations are possible. Here we will discuss the case when $d = \frac{1}{2}$, e.g., the focal spot is in the center of the cell.

If $\chi^{(3)} = \chi'^{(3)} = 0$ only direct FHG exists and $J_1 \equiv J_d$. For infinitely tight focusing, J_d reaches its maximum at $\Delta_{15} = 6/b_1$ [12]. $|J_d|^2$ as a function of $\Delta_{15}L/2$ is plotted in Fig. 8 for $q_1 = 20$. The optimum value for $\Delta_{15}L/2 = 19\pi$ corresponds to $\Delta_{15} \approx 6/b_1$.

When step processes are taken into account the value of J_1 depends on J_s and W . Some consideration of the behavior of J_s will be given. J_s can be presented as a complex number:

$$J_s(\Delta_{135}L/2, \Delta_{13}L/2, q_1) = \text{Re } J_s + i \text{Im } J_s.$$

As seen from (32) the product $WL \text{Im } J_s$ is added to J_d and, depending on the signs, the sum should be $J_d \pm |WL \text{Im } J_s|$. It is easy to prove that the real part can be presented as ($d = \frac{1}{2}$):

$$\text{Re } J_s = \frac{1}{2} \int_{-1}^1 \frac{\exp(-i\Delta_{135}\eta) d\eta}{(1 - iq_1\eta)^2} \int_{-1}^1 \frac{\exp(-i\Delta_{13}\tau) d\tau}{(1 - iq_1\tau)^2} \quad (35)$$

and, making the substitution $x = yq_1$, we obtain for an infinite medium

$$\begin{aligned} \text{Re } J_s &= \frac{1}{2} \int_{-\infty}^{\infty} \frac{\exp(-i\Delta_{135}b_1x/2) dx}{(1 - ix)^2} \\ &\cdot \int_{-\infty}^{\infty} \frac{\exp(-i\Delta_{13}b_1y/2) dy}{(1 - iy)^2} \\ &= \frac{1}{2} \pi^2 b_1^2 \Delta_{13} \Delta_{135} \exp(-b_1 \Delta_{15}/2), \Delta_{135} > 0, \\ &\cdot \Delta_{13} > 0. \\ &= 0, \Delta_{135} \leq 0, \Delta_{13} \leq 0; \quad \text{or } \Delta_{135} \leq 0; \\ &\text{or } \Delta_{13} \leq 0. \end{aligned} \quad (36)$$

The maximum value of $\text{Re } J_s$ is obtained when $\Delta_{13} = \Delta_{135} = 2/b_1$ which corresponds to $\Delta_{15} = 2\Delta_{13} = 4/b_1$. For tight focusing, $\text{Re } J_s$ is negligible when $\Delta_{13} \leq 0$. This is the case for a

mixture of an inert gas and Cd, Zn, or Mg. Δ_{13} is positive for a mixture of an inert gas and an alkali metal.

We did not succeed in finding a simple enough analytical approximation for the function $\text{Im } J_s$. However to obtain a qualitative estimation, the following procedure was adopted. For $d = \frac{1}{2}$, $q_1 = 20$, the integral J_s was numerically calculated using the same technique as for integral (19). Sets of points were found in the plane $(\Delta_{135}L/2, \Delta_{13}L/2)$ with the interval be-

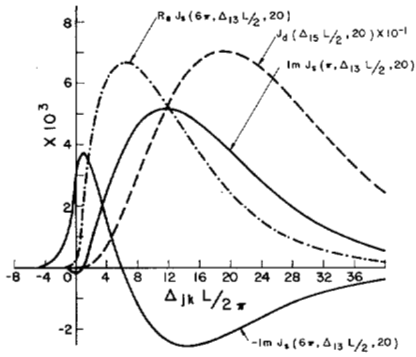


Fig. 8. Functions $J_d(\Delta_{15}L/2, 20)$, $\text{Im } J_s(6\pi, \Delta_{13}L/2, 20)$, $\text{Im } J_s(\pi, \Delta_{13}L/2, 20)$, and $\text{Re } J_s(6\pi, \Delta_{13}L/2, 20)$ versus wave-vector mismatch Δ_{jk} .

tween them $\delta(\Delta_{135}L/2) = \delta(\Delta_{13}L/2) = \pi/2$. Some of the most interesting results are shown in Fig. 8. The behavior of $\text{Re } J_s$ corresponds to the analytical approximation obtained above. $(\text{Re } J_s)_{\text{max}}$ is achieved at $\Delta_{13}L/2 = \Delta_{135}L/2 = 6\pi$. The calculated value of $(\text{Re } J_s)_{\text{max}}$ is 0.37 percent less than the maximum analytical value derived from (36) at $\Delta_{13} = \Delta_{135} = 2/b_1$. In an area where Δ_{13} or Δ_{135} or both of them are negative, $\text{Re } J_s$ has periodic positive and negative values and is at least three orders of magnitude less than its maximum value.

The investigation of $\text{Im } J_s$ shows that the plane $(\Delta_{135}L/2, \Delta_{13}L/2)$ can be divided into three areas:

1) That area defined by inequalities $\Delta_{135} > 0$ and $|\Delta_{13}| < \Delta_{135}$. In this area $\text{Im } J_s < 0$ and reaches its maximum value at the point $\Delta_{135}L/2 = 12\pi$, $\Delta_{13}L/2 = \pi$. $\text{Im } J_s$ as a function of $\Delta_{13}L/2$ at $\Delta_{135}L/2 = \pi$ and $\Delta_{135}L/2 = 6\pi$ is shown in Fig. 8.

2) That area defined by inequalities $\Delta_{13} > 0$ and $|\Delta_{135}| < \Delta_{13}$. In this area $\text{Im } J_s > 0$ and reaches its maximum at the point $\Delta_{135}L/2 = \pi$, $\Delta_{13}L/2 = 12\pi$. The areas 1) and 2) are divided by the diagonal $\Delta_{13} = \Delta_{135}$ on which $\text{Im } J_s = 0$ (Fig. 8). The values of $\text{Im } J_s$ in these two areas are symmetric and

$$[\text{Im } J_s(\Delta_{135}L/2, \Delta_{13}L/2)]_1 = -[\text{Im } J_s(\Delta_{13}L/2, \Delta_{135}L/2)]_2.$$

3) The rest of the $(\Delta_{135}L/2, \Delta_{13}L/2)$ plane is the third area where $\text{Im } J_s$ is changing its sign with variations of the variables and its absolute value is at least three orders of magnitude less than $(\text{Im } J_s)_{\text{max}}$. Other calculations for different q_1 between 10 and 20 show the same behavior. They also permit us to conclude that $\text{Im } J_s(\Delta_{135}L/2, \Delta_{13}L/2)$ has a maximum absolute value at the points $(\Delta_{135}L/2 = \pi, \Delta_{13}L/2 = 4/b_1)$ and $(\Delta_{135}L/2 = 4/b_1, \Delta_{13}L/2 = \pi)$. Some use of this behavior of $\text{Re } J_s$ and $\text{Im } J_s$ may be exploited when the measurement of $\chi^{(5)}$ is performed.

When J_1 is calculated as a function of Δ_{15} (or Δ_{13}) for a specific mixture it should be noted that for every given value of Δ_{15} there is a corresponding exact value of Δ_{13} defined by the dispersion law of the nonlinear medium. To achieve some independence between Δ_{15} and Δ_{13} it is necessary to use a mul-

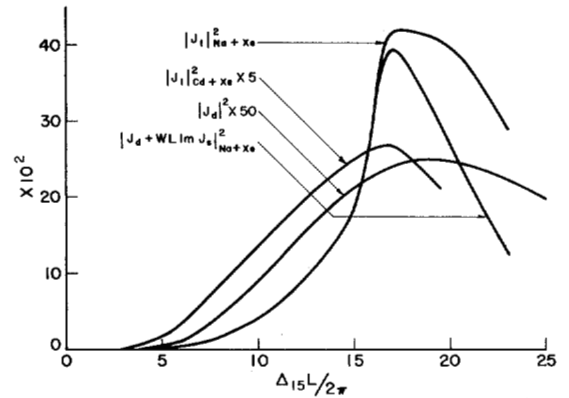


Fig. 9. Optimization of FHG power represented by $|J_1(\Delta_{15}L/2, \Delta_{13}L/2, 20)|^2$ as a function of Δ_{15} for mixture of Na + Xe and Cd + Xe. Functions $|J_d + WL \text{Im } J_s|^2_{\text{Na+Xe}}$ and $|J_d|^2_{\text{Na+Xe}}$ are presented for comparison.

ticomponent gaseous mixture. However, such an approach would involve further practical problems.

The functions $|J_d|^2$, $|J_1|^2$, and $|J_d + WL \text{Im } J_s|^2$ versus $\Delta_{15}L/2$ for a mixture of Na + Xe are plotted in Fig. 9. For this mixture $\Delta_{13} > 0$ when $\Delta_{15} > 0$ and $\text{Im } J_s > 0$. In the same figure, $|J_1|^2$ for Cd + Xe is plotted, for which $\Delta_{13} < 0$ and $\Delta_{15} > 0$. In this case $\text{Re } J_s = 0$ and $\text{Im } J_s < 0$. Because of the different sign of Δ_{13} the ratio

$$|J_1|^2_{\text{Na+Xe}}/|J_1|^2_{\text{Cd+Xe}} \approx 8$$

while

$$|\text{Im } J_s|^2_{\text{Na+Xe}}/|\text{Im } J_s|^2_{\text{Cd+Xe}} \approx 2$$

in their maxima. For both mixtures $W = 6.02 \text{ cm}^{-1}$ and $L = 20 \text{ cm}$ were adopted. With this value of W the fifth harmonic resulting from the step processes is greater than that from the direct process. Hence the maximum of $|J_1|^2$ moves towards lower $\Delta_{15}L/2$ values. The accuracy of these curves is less than that in the other figures because of the step calculations.

V. SUMMARY

In this paper we have discussed the theory of the most promising schemes for FHG of powerful laser radiation. The plane-wave approximation has been applied to the cascade process and also to the scheme employing media with third- and fifth-order susceptibilities, to estimate the maximum conversion efficiency. Comparable efficiencies were found for both schemes.

Expressions for the signal amplitude and the power for four-wave nonlinear processes in Gaussian beams with arbitrary confocal parameters and waist locations have been derived. In the case of FHG, maximum output from the mixing step is obtained for equal confocal parameters of all the interaction beams. Thus a practical system should have a simple arrangement since SHG and THG are also optimized at equal confocal parameters. The analysis of FHG with a focused beam in a nonlinear media with third- and fifth-order susceptibility shows that consideration of interference between step-wise and direct processes is important for fifth-harmonic efficiency. For numerical estimation of various processes more data are neces-

sary, especially the nonlinear susceptibilities. A two-photon resonance will provide substantial enhancement in all nonlinear susceptibilities involved and consequently increase the conversion efficiency of the system.

Finally we note that these results are applicable to FHG with IR lasers using molecular gases as nonlinear media [22], [23]. The relatively weaker dispersion in the IR may pose less technical problems to achieve multistep phase matching.

ACKNOWLEDGMENT

The authors wish to thank J. Curley and R. Fedosejevs for their assistance in the preparation of the numerical programs used in this study.

REFERENCES

- [1] S. E. Harris, J. F. Young, A. H. Kung, D. M. Bloom, and G. C. Bjorklund, "Generation of ultraviolet and vacuum ultraviolet radiation," in *Laser Spectroscopy*, R. G. Brewer and A. Mooradian, Ed. New York: Plenum, 1973, pp. 59-75; see also references.
- [2] D. M. Bloom, G. W. Bekkers, J. F. Young, and S. E. Harris, "Third harmonic generation on phase-matched alkali metal vapors," *Appl. Phys. Lett.*, vol. 26, pp. 687-689, 1975.
- [3] D. M. Bloom, J. E. Young, and S. E. Harris, "Mixed metal vapor phase matching for third-harmonic generation," *Appl. Phys. Lett.*, vol. 27, pp. 390-392, 1975.
- [4] S. E. Harris, "Generation of vacuum-ultraviolet and soft-x-ray radiation using high-order nonlinear optical polarizabilities," *Phys. Rev. Lett.*, vol. 31, pp. 341-344, 1973.
- [5] E. Yablonovitch, C. Flytzanis, and N. Bloembergen, "Anisotropic interference of three-wave and double two-wave frequency mixing in GaAs," *Phys. Rev. Lett.*, vol. 29, pp. 865-868, 1972.
- [6] a) S. A. Akhmanov *et al.*, "Direct and cascade processes in higher optical harmonic generation," in *Abstracts 7th All-Union Conf. Coherent and Nonlinear Optics* (Tashkent, USSR, May, 1974), Moscow, USSR: Moscow State Univ. Press, pp. 15-17. b) S. A. Akhmanov, A. N. Dubovik, S. M. Saltiel, I. V. Tomov, and V. G. Tunkin, "Nonlinear optical effects of fourth order in the field in a lithium formate crystal," *ZhETF Pis. Red.*, vol. 20, pp. 264-268, 1974 (*JETP Lett.*, vol. 20, pp. 117-118, 1974).
- [7] A. G. Akhmanov *et al.*, "Generation of coherent radiation at $\lambda = 2120 \text{ \AA}$ by cascade frequency conversion," *ZhETF Pis. Red.*, vol. 10, pp. 244-249, 1969 (*JETP Lett.*, vol. 10, pp. 154-157, 1969).
- [8] S. G. Dinev, K. V. Stamenov, and I. V. Tomov, "Generation of tunable UV radiation in the range 216-237 nm," *Optics Commun.*, vol. 5, pp. 419-421, 1972.
- [9] V. G. Tunkin, T. Usmanov, and V. A. Shakizov, "Generation of fifth picosecond laser harmonic," *Kvantovaya Electronica*, vol. 11, pp. 117-118, 1972 (*Sov. J. Quant. Electron.*, vol. 2, pp. 487-488, 1973).
- [10] C. R. Vidal and M. M. Hessel, "Heat-pipe oven for homogeneous mixtures of saturated and unsaturated vapors: Application to NaLi," *J. Appl. Phys.*, vol. 43, pp. 2776-2780, 1972.
- [11] M. M. Hessel and T. B. Lucatorto, "The rotating heat-pipe oven: A universal device for the containment of atomic and molecular vapors," *Rev. Sci. Instrum.*, vol. 44, pp. 561-561, 1973.
- [12] Laser Program Ann. Rep., Lawrence Livermore Laboratory, Univ. California, Livermore, CA, UCRL-50021-74, p. 282, 1974.
- [13] J. A. Armstrong, N. Bloembergen, J. Ducuing, and P. S. Pershan, "Interactions between light waves in a nonlinear dielectric," *Phys. Rev.*, vol. 127, pp. 1918-1939, 1962.
- [14] G. D. Boyd and D. A. Kleinman, "Parametric interaction of focused Gaussian light beams," *J. Appl. Phys.*, vol. 39, pp. 3597-3639, 1968.
- [15] J. F. Ward and G. H. C. New, "Optical third harmonic generation in gases by a focused laser beam," *Phys. Rev.*, vol. 185, pp. 57-72, 1969.
- [16] A. P. Sukhorukov and I. V. Tomov, "Wave pattern of third optical harmonic generation in isotropic and anisotropic media," *ZhETF*, vol. 58, pp. 1626-1639, 1970 (*Sov. Phys. JETP*, vol. 31, pp. 872-879, 1970).
- [17] R. B. Miles and S. E. Harris, "Optical third harmonic generation in alkali metal vapors," *IEEE J. Quantum Electron.*, vol. QE-9, pp. 420-483, 1973.
- [18] G. C. Bjorklund, "Effects of focusing on third-order nonlinear processes in isotropic media," *IEEE J. Quantum Electron.*, vol. QE-11, pp. 287-296, 1975.
- [19] F. Abramovici, "The accurate calculation of Fourier integrals by the fast Fourier transform technique," *J. Comput. Phys.*, vol. 11, pp. 28-37, 1973.
- [20] H. Eicher, "Third-order susceptibility of alkali metal vapors," *IEEE J. Quantum Electron.*, vol. QE-11, pp. 121-130, 1975.
- [21] V. M. Mitev and I. V. Tomov, "Nonlinear susceptibility of the fifth-order of alkali metal vapors," presented at the Second Nat. Conf. Young Physicists, Sofia, Bulgaria, Apr. 1974.
- [22] Y. Ueda and K. Shimoda, "Optical third harmonic generation by molecular vibration," *J. Phys. Soc. Japan*, vol. 28, pp. 196-207, 1970.
- [23] C. Y. She and K. W. Billman, "Infrared-pumped third-harmonic and sum-frequency generation in diatomic molecules," *Appl. Phys. Lett.*, vol. 27, pp. 76-79, 1975.
- [24] W. L. Wiese, A. W. Smith, and B. M. Miles, *Atomic Transition Probabilities*, vol. 2. NSRDS-NBS 22, 1969 (sodium through calcium).
- [25] W. R. Newell, K. J. Ross, and J. B. Wickes, *J. Phys. B: Atom. Molec. Phys.*, vol. 4, pp. 684-689, 1971.
- [26] C. J. Mitchell, *J. Phys. B: Atom. Molec. Phys.*, vol. 8, pp. 25-30, 1975.
- [27] W. R. Newell, K. J. Ross, *J. Phys. B: Atom. Molec. Phys.*, vol. 5, pp. 701-709, 1972.